NASA TECHNICAL MEMORANDUM

NASA TM-73,263

NASA TM-73,263

A FLIGHT INVESTIGATION OF THE WAKE TURBULENCE ALLEVIATION RESULTING FROM A FLAP CONFIGURATION CHANGE ON A B-747 AIRCRAFT

Robert A. Jacobsen and Barbara J. Short

Ames Research Center
Moffett Field, Calif. 94035

July 1977

NOMENCLATURE

Physical quantities in this report are given in the International System of Units (SI) and parenthetically in English Measurement Units. The measurements were taken in English Measurement Units. Factors relating the two systems are presented in reference 1.

a_n	normal acceleration at the center of gravity, g units
a_y	lateral acceleration at the center of gravity, g units
AR	aspect ratio
b	wing span, m (ft)
c	wing chord, m (ft)
C_L	lift coefficient, $\frac{\text{lift}}{\bar{q}S}$
C_ℓ	rolling-moment coefficient, $\frac{\text{rolling moment}}{\bar{q}Sb}$
C_m	pitching-moment coefficient, $\frac{\text{pitching moment}}{\bar{q}Sc}$
C_N	normal-force coefficient, $\frac{\text{normal force}}{\bar{q}S}$
C_n	yawing-moment coefficient, $\frac{\text{yawing moment}}{\bar{q}Sb}$
C_Y	lateral-force coefficient, $\frac{\text{lateral force}}{\bar{q}S}$
$d\ell$	elemental rolling moment, N-m (lb-ft)
dr_v	elemental vortex radius, m (ft)
h	test altitude, m (ft)
I_x, I_y, I_z	moments of inertia about the X, Y, Z axes, kg-m^2 (slug-ft^2)
ℓ	rolling moment, N-m (lb-ft)
LF/LF	inboard and outboard engines at thrust for level flight
LF/O	inboard engines at thrust for level flight and outboard engines at idle thrust
O/LF	inboard engines at idle thrust and outboard engines at thrust for level flight

p	roll velocity, deg/sec
$\dot{p}$	roll acceleration, rad/sec^2
P	semiperimeter parameter
q	pitch velocity, deg/sec
$\dot{q}$	pitch acceleration, rad/sec^2
$\bar{q}$	dynamic pressure, N/m^2 (lb/ft^2)
r	yaw velocity, deg/sec
$\dot{r}$	yaw acceleration, rad/sec^2
r_v	vortex radius, m (ft)
S	wing area, m^2 (ft^2)
V	true airspeed, knots or m/sec (ft/sec)
V_θ	vortex tangential velocity, m/sec (ft/sec)
W	gross weight of aircraft, N (lb)
X,Y,Z	body axes of Learjet
α	angle of attack, deg
β	angle of sideslip, deg
β_v	vortex core size parameter, 1/m^2 (1/ft^2)
δ_a	total aileron deflection angle, deg
δ_e	elevator deflection angle, deg
δ_r	rudder deflection angle, deg
Γ	circulation, m^2/sec (ft^2/sec)
η	angle of intercept with vortex, deg
ρ	air density, N-sec^2/m^4 (lb-sec^2/ft^4)
ϕ	roll angle, deg
$\dot{\Omega}$	spin control ratio (eq. 6)
30/1	inboard flaps deflected 30° and outboard flaps deflected 1°

30/30 inboard and outboard flaps deflected 30°

Subscripts:

c	calculated
f	following aircraft
g	generating aircraft
max	maximum
mc	maximum control
o	equilibrium
p	partial derivative with respect to $\frac{pb}{2V}$
q	partial derivative with respect to $\frac{qc}{2V}$
r	partial derivative with respect to $\frac{rb}{2V}$
v	vortex
α	partial derivative with respect to α
β	partial derivative with respect to β
δ_a	partial derivative with respect to δ_a
δ_e	partial derivative with respect to δ_e
δ_r	partial derivative with respect to δ_r
l	vortex core

A FLIGHT INVESTIGATION OF THE WAKE TURBULENCE ALLEVIATION RESULTING FROM A FLAP CONFIGURATION CHANGE ON A B-747 AIRCRAFT

Robert A. Jacobsen and Barbara J. Short

Ames Research Center

SUMMARY

A flight test investigation has been conducted to evaluate the effects of a flap configuration change on the vortex wake characteristics of a Boeing 747 (B-747) aircraft as measured by differences in upset response resulting from deliberate vortex encounters by a following Learjet aircraft and by direct measurement of the velocities in the wake. The flaps of the B-747 have a predominant effect on the wake. The normal landing flap configuration produces a strong vortex that is attenuated when the outboard flap segments are raised; at that point, however, extension of the landing gear increases the vortex-induced upsets. These effects are in general agreement with existing wind tunnel and flight data for the modified flap configuration; however, the previously measured adverse effects of increased lift coefficient and idle thrust are not readily evident.

INTRODUCTION

The wake vortices generated by transport aircraft have been of concern because of the potential hazard they impose on following aircraft. The wakes of heavy jet transports are of particular interest since the intensity of the vortex produced is a direct function of gross weight. Protection from the hazard presented by these wakes is provided by imposing minimum separation distances between aircraft on the same approach path. Separation between the aircraft allows time for the vortices generated by the first aircraft to dissipate before the second one passes through the same airspace. Anticipated increases in air traffic make it desirable to reduce the minimum separation distance required to provide a higher rate of terminal area operations.

Two approaches for reducing the minimum separation requirements have been under investigation recently. The first approach is to develop procedures for avoiding vortex encounters, and the second is to develop aircraft configurations which minimize the hazard associated with a vortex encounter. The Department of Transportation is responsible for investigating techniques for avoiding vortex encounters, thereby allowing reduced separation distances. This approach is based on a knowledge of vortex behavior and the ability to predict when no vortex will be present on the approach path. To update the predicted vortex motion it is necessary to monitor the locations

of the vortices. This requirement has led to considerable research and development work in ground-based vortex detection equipment.

The National Aeronautics and Space Administration is responsible for developing aircraft configurations which produce less hazardous wakes. This technique results in reduced minimum separation requirements by reducing the upset associated with a vortex encounter. The subject of this report is a flight evaluation of an altered flap scheduling technique on a B-747 designed to reduce the hazard associated with its wake. The technique was discovered and developed in the ground-based facilities at Ames Research Center and Langley Research Center. Wind-tunnel tests (refs. 2-4) showed that raising the outboard flap segment significantly reduced the rolling moment induced on a following model.

Three aircraft were used in a flight research program conducted at NASA's Dryden Flight Research Center to verify the ground-based test results. A Learjet operated by NASA's Ames Research Center and a T-37B operated by NASA's Dryden Flight Research Center were used to probe the wake of NASA's B-747. Measurements of the upset from the wake encounters were made by both probe aircraft, and measurements of the velocity profiles of the wake of the B-747 were made by the Learjet. This report documents the upsets induced by the B-747 wake on the Learjet and the velocity profiles measured. The results obtained by the T-37B were reported in reference 5.

TEST DESCRIPTION

Test Aircraft

The B-747 aircraft (fig. 1) used as a wake generating airplane for this investigation was modified to allow the inboard and outboard flap segments to be extended independently. Smoke generators were mounted on each wing tip, at the outboard edge of the outboard flap and at the outboard edge of the inboard flap. A modified DME (Distance Measuring Equipment) unit was installed in the aircraft to allow direct measurement of the range to the probe aircraft. A physical description of the B-747 is given in table 1.

The Learjet probe aircraft (fig. 2) was instrumented to measure the pertinent parameters, including the aircraft motions and its control surface deflections. Airspeed, altitude and angles of attack and sideslip were measured by an instrumented boom on the nose of the aircraft. A three-component hot-wire anemometer was also mounted on the nose boom of the aircraft for measuring the velocities in the wake. The data were recorded on magnetic tape on board the aircraft. The response measurements to document the upset resulting from an encounter were recorded in digital form, while the hot-wire anemometer measurements were recorded in analog form because of their high-frequency content. A physical description of the Learjet is also given in table 1. A more complete description of this flight test technique is given in reference 6.

Test Conditions

The flight tests on the B-747 were conducted at an altitude of approximately 3800 m (12,500 ft) at airspeeds ranging from 150 knots indicated airspeed (KIAS) to 180 KIAS. The gross weight of the B-747 ranged from 217,000 to 272,000 kg (480,000 to 600,000 lb). The lift coefficient varied from 1.0 to 1.4. The configurations that were tested are presented in table 2. The configuration used as a basis for comparison was the normal B-747 landing configuration with both the inboard and outboard flap segments deflected 30° (30/30). The vortex minimization configuration investigated was one with the inboard flap segment at 30° and the outboard segment at 1° (30/1). The 1° deflection was required operationally to enable the leading edge protection devices to be extended.

Flight Test Procedures

Two separate flight test procedures are used to obtain the upset and velocity profile data. Some aspects of the two procedures are similar. For each configuration being studied the wake is encountered at a separation distance which is large enough to assure safety. Data are then obtained at decreasing distances until a predetermined minimum distance is reached or until the continued reduction of separation distance is judged to be hazardous either by the pilot or through assessment of the loads imposed on the aircraft.

In making measurements of the upset when encountering the wake, the flight test procedure used is to fly the probe aircraft along the axis of a vortex which has been made visible through the injection of smoke. The motion resulting from the imposed moments is then measured. Since the severity of an encounter depends strongly on the location of the vortex relative to the probe aircraft, a large number of encounters is required to insure that the maximum upsets possible are received. Once the data from this large number of upsets have been reduced, an upper bound (or envelope) to the data is constructed and is assumed to represent the maximum upset that the wake produces on the probe aircraft.

To measure the velocity profiles of the wake, the flight procedure used is to fly the probe aircraft across the wake, attempting to penetrate the core of the vortex with the nose boom. As in making upset measurements, the location of the vortex relative to the probe path has a large effect on the resulting data. In this case, however, the displacement of the vortices is accounted for in the data reduction process. A number of passes across the wake is made to insure that adequate penetration of the vortex has occurred. The data from each pass are then reduced independently.

DATA ANALYSIS OF RESULTS

Upset Measurements

The data for determining the vortex imposed upsets of the probe aircraft were reduced in a manner depicted by the block diagram of figure 3. The airborne data are conditioned and recorded aboard the aircraft. After the flight, instrument calibration factors are applied. Effective angles of attack and sideslip are computed and used along with the recorded control inputs to determine the accelerations that would have been imposed in the absence of the vortex itself. The difference between these computed accelerations and those measured are due to the vortex flow field.

Figure 4 shows representative time histories of measured responses of the Learjet flying in the wake of the B-747 airplane. It is evident that the Learjet experienced appreciable disturbances about all three axes as a region of vortex flow was encountered at about 4 sec. The responses are the combined result of the vortex and the pilot's control inputs.

To extract the upsets induced by the vortex encounter from the total measured upsets, the roll, pitch, and yaw accelerations due to the aircraft aerodynamics, $\dot{p}_c$, $\dot{q}_c$, and $\dot{r}_c$, were calculated and subtracted from the measured accelerations, $\dot{p}$, $\dot{q}$, and $\dot{r}$. Thus the vortex-induced accelerations are

$$\dot{p}_v = \dot{p} - \dot{p}_c \tag{1a}$$

$$\dot{q}_v = \dot{q} - \dot{q}_c \tag{1b}$$

$$\dot{r}_v = \dot{r} - \dot{r}_c \tag{1c}$$

where

$$\dot{p}_c = \frac{\bar{q}Sb}{I_x}\left[C_{\ell_\beta}\beta_c + C_{\ell_{\delta_a}}\delta_a + C_{\ell_{\delta_r}}\delta_r + \frac{b}{2V}\left(C_{\ell_p}p + C_{\ell_r}r\right)\right] \tag{2a}$$

$$\dot{q}_c = \frac{\bar{q}Sc}{I_y}\left[C_{m_o} + C_{m_\alpha}\alpha_c + C_{m_{\delta_e}}\delta_e + \frac{c}{2V}\left(C_{m_q}q\right)\right] \tag{2b}$$

$$\dot{r}_c = \frac{\bar{q}Sb}{I_z}\left[C_{n_\beta}\beta_c + C_{n_{\delta_a}}\delta_a + C_{n_{\delta_r}}\delta_r + \frac{b}{2V}\left(C_{n_p}p + C_{n_r}r\right)\right] \tag{2c}$$

The aircraft characteristics and aerodynamic coefficients about the body axes of the Learjet are listed in table 3. The coefficients were determined from the results of flight and wind-tunnel tests (refs. 7-9).

The angles, α_c and β_c, used in equations (2) were determined from the measured normal and lateral accelerations through the relationships

$$\alpha_c = \frac{Wa_n}{C_{N_\alpha} \bar{q} S} \tag{3a}$$

$$\beta_c = -\frac{Wa_y}{C_{y_\beta} \bar{q} S} \tag{3b}$$

These angles represent effective angles of attack and sideslip for use in computing aerodynamic moments on the aircraft from equations (2). As expected, they differ from those angles measured at a single point in the flow field by the flow direction vanes mounted on the nose boom. Comparison of the calculated values with the vane measurements for the encounter shown in figure 4 are indicated in figure 5. As can be seen, the use of equations (3) suppresses the transient responses that are independent of aircraft motion. Prior to vortex encounter, the values of α_c are about 2° lower than the measured values. This difference is not a common occurrence, and, in general, the calculated values provide accurate time histories of the effective aircraft angles. The pitching-moment coefficient required to trim the aircraft, C_{m_0}, in equation (2b) is determined with the use of equation (3a) for the case of $a_n = 1$ g.

Comparisons of the measured, calculated, and vortex-induced accelerations for the encounter shown in figure 4 are shown in figure 6. The maximum accelerations induced by the vortex are of greater magnitude than those measured; a typical situation when the pilot's control inputs moderate the excursions of the Learjet during the vortex encounter.

In references 9 and 10, it is shown that the rolling-moment control ratio, the vortex-induced roll acceleration divided by the maximum available roll acceleration due to control input, is a useful parameter for the determination of minimum safe separation distances between generating and following aircraft. In the nomenclature of this report, the rolling-moment control ratio is $\dot{p}_v/\dot{p}_{mc}$, where

$$\dot{p}_{mc} = \frac{\bar{q} S b}{I_x} C_{\ell_{\delta_a}} \delta_{a_{max}} \tag{5}$$

Figure 4 shows that the aircraft encountering a vortex can be subjected to appreciable upsets in pitch and yaw as well as in roll. To account for the combined axes upsets, the normalized pitch and yaw accelerations can be combined with the roll acceleration to obtain a total spin control ratio

$$\dot{\Omega} = \sqrt{\left(\frac{\dot{p}_v}{\dot{p}_{mc}}\right)^2 + \left(\frac{\dot{q}_v}{\dot{q}_{mc}}\right)^2 + \left(\frac{\dot{r}_v}{\dot{r}_{mc}}\right)^2} \tag{6}$$

The pitch and yaw accelerations with maximum controls are

$$\dot{q}_{mc} = \frac{\bar{q}Sc}{I_y} C_{m_{\delta_e}} \delta_{e_{max}} \tag{7a}$$

and

$$\dot{r}_{mc} = \frac{\bar{q}Sb}{I_z} C_{m_{\delta_r}} \delta_{r_{max}} \tag{7b}$$

A comparison of the spin control ratio, $\dot{\Omega}$, with the rolling-moment control ratio, $\dot{p}_v/\dot{p}_{mc}$, is shown in figure 7 for the Learjet behind the B-747 with flaps down 30/30, gear up, and thrust for level flight, at $C_L = 1.4$. When the encounter is near the core of the vortex, as evidenced by the larger control ratios, the combined axes upsets are not significantly greater than the roll upsets alone, the average increase being about 5 percent. When the encounter is closer to the edge of the vortex (i.e., lower values of the control ratio) the measurements indicate large upsets can occur in the pitch and yaw axes and they should be included in the probe aircraft response measurements. It is speculated that the spin control ratio would be a more adequate measurement of the response for a nonaxial wake encounter.

The vortex-induced upsets were measured to evaluate the effects of changes in the generating aircraft configuration. The B-747 configurations investigated are listed in table 2 along with the flight conditions. The velocity of the probe aircraft was usually higher than the velocity of the B-747. To eliminate the effect of this velocity difference, the measured responses were corrected to the velocity of the generating aircraft. Figures 8 to 12 show the effects of the B-747 configuration changes on the responses of the probe aircraft.

The vortex-induced upset responses of the Learjet determined for several values of B-747 lift coefficient, C_L, are shown in figure 8, where the vortex-induced rolling moment coefficient, C_{ℓ_v}, is plotted as a function of separation distance between the generating and the probe aircraft. The level of maximum roll control power is included in the figure to give an indication of the rolling-moment control ratio. The rolling-moment control ratio in terms of rolling-moment coefficient is given by

$$\frac{\dot{p}_v}{\dot{p}_{mc}} = \frac{C_{\ell_v}}{C_{\ell_{\delta_a}} \delta_{a_{max}}} \tag{8}$$

Even though it might be expected that the higher lift coefficients of the B-747 would produce larger upsets because of the increased circulation in the vortices, no effect of the change in C_L from 1.0 to 1.4 is discernible for either the normal landing flap (30/30) configuration (fig. 8(a)) or the configuration with the outboard flap segment retracted (30/1) (fig. 8(b)).

This result disagrees with the wind-tunnel results reported in reference 2 but agrees with the T-37 flight test results in reference 5 that indicate C_L has little effect on the vortex of the B-747 aircraft at operational separation distances in the flaps down (30/30) configuration (fig. 8(a)). The results reported in reference 5 do show, however, that an increase of C_L from 1.2 to 1.4 does have a strong adverse effect on the vortex of the B-747 with the outboard flaps up 30/1. This effect is not evident in the present results shown in figure 8(b) where the maximum level of upset measured near 5 km (2.7 n. mi.) is only slightly less for $C_L = 1.0$ than 1.4. Although no upset measurements were taken with $C_L = 1.2$ at the same separation distance for direct comparison with reference 5, it seems unlikely that the level of upset would be greatly reduced at this intermediate lift coefficient.

The data of figures 8 are replotted in figure 9 to show the effect of the B-747 flap configuration. The data show that the vortex encounter was more severe behind the 30/30 flap configuration and was still roughly equivalent to the 30/1 flap configuration at more than twice the separation distance. Included in the figure are the wind-tunnel data from references 2 and 11. The flight test results confirm the alleviation of the vortex strength with the B-747 outboard flaps up 30/1 as measured in the wind tunnel at a scaled separation distance of 0.85 km (0.5 n. mi.). The flight-test results, however, do not show the increase in C_{ℓ_v} with lift coefficient that was measured in the wind tunnel.

The adverse effect of extending the landing gear on the 30/1 flap configuration is shown in figure 10. This effect is also shown in the data of reference 5. Included for comparison in figure 10 is a dashed line that indicates the upper boundary of the data in figure 8(a) for the gear up, 30/30 flap configuration. The effect of the deflected outboard flap is greater than the effect of the landing gear, and both configuration changes increase the magnitude of the upset responses.

The effect of the B-747 engine thrust is shown in figures 11. The upset response data are shown for three engine thrust settings: all engines at level flight thrust (LF/LF) (figs. 8), the inboard engines at idle thrust with the outboard engines at level flight thrust (O/LF), and the inboard engines at level flight thrust with the outboard engines at idle thrust (LF/O). In general, it appears that the vortex encounter is more severe behind the 30/30 flap configuration (fig. 11(a)) with engines idle than with all engines at level flight thrust; this effect is not evident behind the 30/1 flap configuration (fig. 11(b)), however. No definitive difference is apparent between the configuration with inboard engines idle and the configuration with outboard engines idle. In the present investigation no measurements were taken with all engines at idle thrust; the results reported in reference 5, however, indicate a strong adverse effect with all engines idle for both flap configurations.

The effect of sideslip angle of the B-747 in the 30/1 flap configuration is shown in figure 12. The sideslip angles were approximately ±2°. Larger

upsets were measured for the case of positive sideslip than for either zero or negative sideslip. It is not known which wing vortex was penetrated during each encounter. Though data are available for only a limited range of separation distances, they indicate that the resulting upset is approximately 50 percent greater with sideslip than for a comparable separation distance with no sideslip. This agrees with the results presented in reference 5 where a larger range of flight conditions was studied.

Velocity Profile Measurements

The velocities in the flow field encountered by the probe aircraft were measured by a three-component hot-wire anemometer probe mounted on the nose boom. The probe aircraft's dynamic response resulting from encountering the wake was measured using angular and linear accelerometers and angular rate and attitude gyros.

The data reduction process to extract the velocity information is indicated by the flow chart of figure 13. The airborne-recorded analog data are digitized at the rate of 1000 samples/sec. (This rate is necessary because of the high-frequency content of the data.) The wake velocities are first computed from the hot-wire data in an axis system aligned with the body axes of the aircraft, and allowances are made for the vertical velocity and pitch rate of the aircraft. The apparent vertical and lateral velocities resulting from the effective angles of attack and sideslip generated as the aircraft reacts to the induced forces are also accounted for. The three components of velocity are then resolved into an axis system aligned with the axis of the vortex using the relative heading for each pass across the wake. The flight path of the probe is computed from the initial airspeed and the measured vertical accelerations and pitching excursions. In this way a velocity distribution along a known path in space is determined.

The velocity profile measured at a separation distance of 5.4 km (2.9 n. mi.) behind the B-747 in its normal landing configuration is shown in figure 14. All three components of velocity are shown: the top one is the vertical velocity defined as positive upward, the middle trace is the lateral component defined as positive to the left of the aircraft that generated the wake, and the bottom trace is the axial velocity component defined as positive toward the aircraft that generated the wake. Data similar to that of figure 14 were measured at a separation distance of 4.1 km (2.2 n. mi.) for the B-747 with its outboard flap segments retracted (?' _) and are shown in figure 15. Although the velocities are shown to be reduced, care must be taken in interpreting these results since the velocity measured depends strongly on the probe path relative to the centers of the vortices.

One method of making direct comparisons that eliminates differences caused by variation in the probe path relative to the vortices is to match the measurements to a mathematical model of the vortex pair and base comparisons on the maximum tangential velocities computed from the models. This method has been adopted for the analysis of the velocity measurements,

and the vortex model provides an estimate of the velocity everywhere in the flow field based on the data from one pass of the probe. The vortex system may initially consist of more than a single pair of vortices; however, the wake model used in this analysis consists of a single pair which implies the assumption that merger of all vortices to a single pair is complete at the separation distances where the measurements were made.

The mathematical model of a single vortex used in the matching process is due to Lamb (ref. 12), and can be written $V_\theta = \frac{\Gamma}{2\pi r_v}(1 - e^{-\beta_v r_v^2})$, where the potential solution, $\frac{\Gamma}{2\pi r_v}$, is modified by an exponential function $e^{-\beta_v r_v^2}$, and β_v is a parameter related to core size. For a vortex pair, the vector sum of the tangential velocities of a pair of Lamb vortices is taken. The vertical and lateral components of velocity due to the modeled pair are computed along the probe flight path, and the model parameters are adjusted to match the measured velocities in the least squares sense. The model parameters are the lateral and vertical coordinates of the two vortices, the vortex strength, and the parameter related to core size (β_v). An initial estimate of these six parameters is made, and an iterative procedure is used to converge on the values of those parameters that provide the best fit. The quality of this matching procedure is shown in figure 16 for the data of figure 14 where the vertical and lateral components of velocity in the wake as computed from the mathematical model are compared with the measured velocities. The model represents the peak velocities reasonably well; in some regions of the flow field, however, the velocities are not well represented.

There are a number of possible reasons for the differences. First, the wake may contain more than a single pair of vortices. Some attempts were made to develop a technique for estimating the locations and parameters for more than a single pair, but it was found that the method generally would not converge to a solution even when the data to be matched was generated by perfect Lamb vortices. Second, the Lamb model probably does not represent the actual velocity distribution in the region of the vortex core. The choice of the Lamb model was dictated by the necessity of having a tractable expression for computation. Finally, it is assumed that the vortex pair is symmetrical, whereas observation in the far wake (see refs. 9 and 13) and results such as those shown in figure 14 for the axial velocity indicate that the assumption is not necessarily valid.

The method consistently provides a good representation of the maximum measured tangential velocities. The decay of the vortices with distance from the generating aircraft and the effect of raising the outboard flap can be seen by observing the change in the peak tangential velocity as given by the vortex models matched to the data. This parameter is plotted against downstream distance in figure 17 where both variables have been normalized in the manner suggested by Iverson (ref. 14). It is evident from these results that there is considerable difference in the maximum velocity from one penetration to the next at comparable distances. This might be due to changes in vortex structure such as those indicated in the photographs of marked vortices shown in reference 9, where local "bursting" can be seen as soon as 10 sec after the wake was generated.

Iverson's correlation has been demonstrated to collapse the data from many sources to a single curve. The mean line through the data correlated by Iverson has been shown in figure 17; it is evident that the dimensionless maximum velocities for the 30/30 flap configuration are representative of values for other aircraft used in the correlation. The results show a marked reduction in peak tangential velocity when the outboard flap is retracted, which is consistent with the response measurements.

Comparison of Velocity Profile Data with Response Data

A technique for determining the peak tangential velocity in the vortex based on measured aircraft response has been developed (see appendix A). This technique allows the results of response measurements to be compared with velocity profile measurements and affords an estimate of the velocity decay at greater separation distances than those for which direct velocity measurements were made. The inverse of the technique also permits estimates of the rolling moment that might be imposed on any encountering aircraft of interest.

The maximum velocity estimation technique was applied only to encounters representing the envelope of the rolling moment data shown in figure 9, and the results are compared with the direct velocity measurements in figure 18. At the smaller values of the dimensionless distance parameter for which response data were available, the estimated velocities are in reasonable agreement with the direct measurements. However, as the separation distance is increased beyond the range of the velocity data, the estimated velocities indicate a more rapid decay with increasing separation distance. This change in slope is reflected in the boundary lines drawn in the figure. These lines indicate that rapid decay begins at a value of the dimensionless distance parameter of about 800 when both flap segments were lowered (30/30) and that the tangential velocity obeys an X^{-2} law rather than the $X^{-1/2}$ law shown by Iverson at lower values of the dimensionless distance parameter.

When the outboard sections of the flaps are raised (30/1), the dimensionless distance at which rapid decay begins is reduced to about 500. Thus, the improvement observed in the response of the probe aircraft due to raising the outboard flap segments is due to two sources. The first can be identified with the reductions at small aircraft separations that were originally observed in ground-based facility tests. The second is a reduction in the separation distance at which a more rapid decay commences. This latter effect is sufficient to more than double the ratios of the peak tangential velocities of the two configurations as the dimensionless distance increases from about 500 to 800. These dimensionless distances correspond to separations of about 2.6 km and 8.3 km (2.5 and 4.5 n. mi.) for the B-747.

The point at which the decay rate changes is based on a limited set of data. It would be expected that this point would depend on atmospheric conditions, particularly turbulence.

CONCLUDING REMARKS

A flight test investigation has been conducted to determine the effects of configuration changes of the B-747 aircraft on its vortex wake as measured by an instrumented probe aircraft through the upset responses experienced and through measurements of the wake velocities encountered. The results of this investigation can be summarized as follows.

1. The flight test results substantiate the wind-tunnel results and previous flight test results that show an alleviation of vortex strength with the B-747 outboard flaps deflected 1° (30/1) as compared with both the inboard and outboard flaps deflected 30° (30/30).

2. The flight test results do not show the adverse effect on the vortex due to an increase in the lift coefficient of the B-747 for the outboard flap retracted (30/1) case as was measured in the wind tunnel and previously in flight.

3. Extension of the landing gear on the 30/1 flap configuration results in more severe upsets; the upsets are not as great as those experienced with the B-747 in normal landing configuration (30/30) with gear retracted, however.

4. A partial reduction in engine thrust of the B-747 has no effect on the vortex of the 30/1 flap configuration and an adverse effect on the vortex of the 30/30 flap configuration.

5. The flight test data show an adverse effect of sideslip angle on the B-747 vortex wake when the outboard flap is retracted (30/1).

6. The velocity profile measurements show that raising the outboard flap segment on the B-747 substantially reduces the peak tangential velocities.

7. The velocity profile data and the velocities derived from the upset data agree well with the $X^{-1/2}$ decay rate indicated by Iverson (ref. 14). However, at the larger separation distances the existence of a change in the decay rate to an X^{-2} law is indicated.

APPENDIX A

ESTIMATION OF VORTEX VELOCITY FROM PROBE AIRCRAFT RESPONSE MEASUREMENTS

The procedure is based on the following assumptions:

1. The envelope of the maximum observed probe-aircraft vortex-induced acceleration represents the condition where the aircraft is centered in the vortex.

2. The velocity distribution can be represented by a single vortex with a distribution of circulation as given by Iverson (ref. 14) for variable eddy viscosity.

3. The rolling moment can be computed from a known velocity distribution using strip theory.

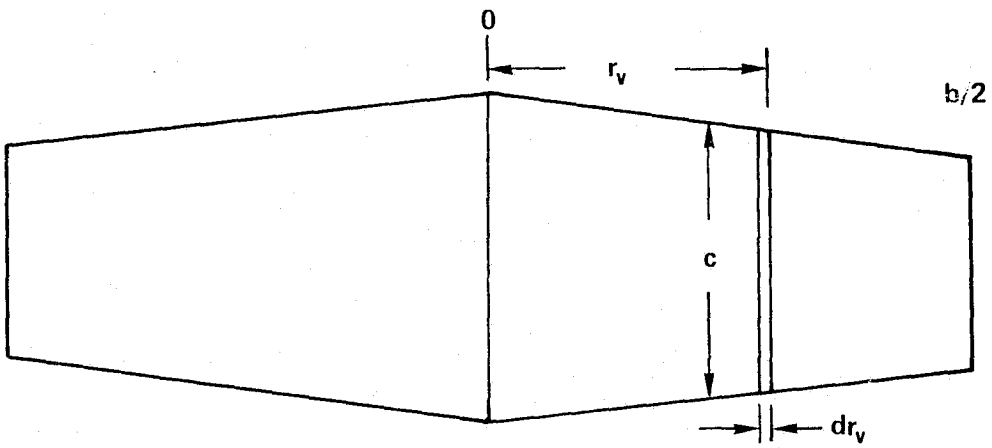

The rolling moment on the element of wing area cdr_v is given by

$$d\ell = C_{L_\alpha} \alpha_v \bar{q}_f c r_v dr_v \tag{A1}$$

where

$$\alpha_v = \frac{V_\theta}{V_f}$$

$$C_{L_\alpha} = \frac{2\pi AR}{PAR + 2}$$

$$V_\theta = \frac{\Gamma(r_v)}{2\pi r_v} \tag{A2}$$

where the semiperimeter parameter, P, and the aspect ratio are based on the wing semispan (ref. 15), and $\Gamma(r_v)$ corresponds to the variable eddy viscosity solution given by Iverson (ref. 14).

The rolling moment for both wing panels is then given by:

$$\ell = \frac{4}{\pi} \frac{W_g b_f^2}{b_g} \left(\frac{\rho_f V_f}{\rho_g V_g}\right) \left[\frac{1}{b_f^2} \left(\frac{AR}{PAR + 2}\right) \int_o^{b/2} \frac{\Gamma(r_v)}{\Gamma_o} c dr_v\right] \tag{A3}$$

where the large radius circulation is assumed to correspond to an elliptically loaded wing, that is,

$$\Gamma_o = \frac{4}{\pi} \frac{W_g}{\rho_g b_g V_g}$$

The dimensionless parameter in the brackets is dependent upon the wing planform and the variation of circulation strength with distance from the center of the vortex. The dimensionless parameter can be expressed in terms of vortex core radius for a given variation of circulation strength. The variation used in the reduction of the data, based on the variation of circulation with radial distances according to Iverson, is shown in figure 19.

The rolling accelerations measured in flight, along with known values of the probe aircraft moment of inertia about the roll axis and generating aircraft weight, velocity, wing-span and altitude, can be used to deduce the value of the dimensionless planform parameter from equation (A3). From this parameter the value of the core radius can be determined (fig. 19). Then

$$V_{\theta_{max}} = \frac{4\Gamma_o}{2\pi r_{v_1}} \tag{A4}$$

according to the variation of Γ with radius given in reference 14.

REFERENCES

1. Mechtly, E. A.: The International System of Units-Physical Constants and Conversion Factors. NASA SP-7012, 1964.

2. Corsiglia, V. R.; Rossow, V. J.; and Ciffone, D. L.: Experimental Study of the Effect of Span Loading on Aircraft Wakes. NASA TM X-62,431, May 1975.

3. Corsiglia, V. R.; and Orloff, K. L.: Scanning Laser-Velocimeter Surveys and Analysis of Multiple Vortex Wakes of an Aircraft. NASA TM X-73,196, Aug. 1976.

4. Dunham, E. R., Jr.: Model Tests of Various Vortex Dissipation Techniques in a Water Towing Tank. Langley Working Paper, LWP-1146, Jan. 1974.

5. Smith, Harriet J.: A Flight Test Investigation of the Rolling Moments Induced on a T-37B Airplane in the Wake of a B-747 Airplane. NASA TM X-56,031, 1975.

6. Jacobsen, R. A.; and Barber, M. R.: Flight Test Techniques for Wake Vortex Minimization Studies. NASA SP-409, 1976, pp. 191-217.

7. Soderman, P. T.; and Aiken, T. N.: Full-Scale Wind-Tunnel Tests of a Small Unpowered Jet Aircraft with a T-Tail. NASA TN D-6573, 1971.

8. Robinson, G. H.; and Larson, R. R.: A Flight Evaluation of Methods for Predicting Vortex Wake Effects on Trailing Aircraft. NASA TN D-6904, 1972.

9. Kurkowski, R. L.; Barber, M. R.; and Garodz, L. J.: Characteristics of Wake Vortex Generated by a Boeing 727 Jet Transport During Two-Segment and Normal Approach Flight Paths. NASA TN D-8222, 1976.

10. Andrews, W. H.; Robinson, G. H.; and Larson, R. R.: Exploratory Investigation of Aircraft Response to the Wing Vortex Wake Generated by Jet Transport Aircraft. NASA TN D-6655, 1972.

11. Rossow, V. J.; Corsiglia, V. R.; and Phillippe, J. J.: Measurements of the Vortex Wakes of a Subsonic- and a Supersonic-Transport Model in the 40- by 80-Foot Wind Tunnel. NASA TM X-62,391, 1974.

12. Lamb, Sir Horace: *Hydrodynamics*, Sixth Edition; Dover Publications, New York, N.Y., 1945.

13. Garodz, L. J.; Hanley, W. J.; and Miller, N. J.: Abbreviated Investigation of the Douglas DC-10 Airplane Vortex Wake Characteristics in Terminal Area-Type Operations. FAA/NAFEC Data Report, Task No. FS-2-73, Aug. 1972.

14. Iverson, J. D.: Correlation of Turbulent Trailing Vortex Decay Data. AIAA Journal of Aircraft, vol. 13, no. 5, May 1976.

15. Rossow, V. J., et al.: Velocity and Rolling-Moment Measurements in the Wake of a Swept Wing Model in the 40- by 80-Foot Wind Tunnel. NASA TM X-62,414, April 1975.

TABLE 1.- AIRCRAFT PHYSICAL CHARACTERISTICS

(a) B-747, wake generator aircraft

Length, m (ft)	70.51 (231.33)
Height, m (ft)	19.33 (63.42)
Wing:	
Area, m^2 (ft^2)	511 (5,500)
Span, m (ft)	59.64 (195.67)
Aspect ratio	6.96
Sweep at quarter chord, deg	37.5
Mean aerodynamic chord, m (ft)	8.33 (27.32)
Incidence angle, deg	2
Dihedral angle, deg	7
Taper ratio	0.356
Control surfaces:	
Rudder area, m^2 (ft^2)	22.9 (247)
Rudder deflection, deg	15
Elevator area, m^2 (ft^2)	32.5 (350)
Elevator deflection, deg	-23 to 17
Aileron area (total), m^2 (ft^2)	20.9 (222)
Aileron deflection, deg	
Inboard	20
Outboard	-25 to 15
Spoiler area (total), m^2 (ft^2)	30.8 (331)
Spoiler deflection, deg	
Panels 6 to 8	20
Panels 1 to 4, 9 to 12	45
Trailing-edge flap area (total), m^2 (ft^2)	78.7 (847)
Trailing-edge flap deflection, deg	30
Leading-edge flap area (total), m^2 (ft^2)	48.1 (518)
Weight, kg (lb):	
Empty	158,220 (348,816)
Maximum takeoff	322,050 (710,000)

TABLE 1.- AIRCRAFT PHYSICAL CHARACTERISTICS - Concluded

(b) Learjet 23 wake probe aircraft

Length, m (ft)	13.18 (43.25)
Height, m (ft)	3.83 (12.58)
Wing:	
Area, m^2 (ft^2)	21.6 (232.0)
Span, m (ft)	10.84 (35.58)
Aspect ratio	5.46
Sweep at 25 percent chord, deg	13.0
Mean aerodynamic chord, m (ft)	2.0 (6.55)
Control surfaces:	
Rudder area, m^2 (ft^2)	0.67 (7.18)
Rudder deflection, deg	30.0
Elevator area, m^2 (ft^2)	1.31 (4.13)
Elevator deflection, deg	14.0
Aileron area, m^2 (ft^2)	1.08 (11.70)
Aileron deflection, deg	20.0
Wing flap area, m^2 (ft^2)	3.42 (36.85)
Wing flap deflection, deg	40.0
Weight, kg (lb):	
Empty	3300 (7275)
Takeoff	6124 (13,500)
Moments of inertia, kg-m^2 (slug-ft^2):	
Roll (empty)	8634 (6364)
Roll (full)	35,112 (25,880)
Pitch (empty)	22,258 (16,405)
Pitch (full)	26,765 (19,728)
Yaw (empty)	28,704 (21,157)
Yaw (full)	66,586 (49,079)

TABLE 2.- AIRCRAFT CONFIGURATIONS AND FLIGHT CONDITIONS

Wake generating aircraft, B-747							Wake probe aircraft, Learjet		
Flaps, deg	Gear	Thrust	β, deg	C_L	V, knots	$W\times10^{-3}$, kg (lb)	$h\times10^{-3}$, m (ft)	V, knots	$W\times10^{-3}$, kg (lb)
30/30	Up	LF/LF	0	1.4	186	272 (599)	3.84 (12.6)	180-214	5.40 (11.9)
				1.3	189	253-269 (557-593)	3.84-4.45 (12.6-14.6)	178-233	4.63-5.18 (10.2-11.4)
				1.2	202	276 (608)	3.81 (12.5)	188-227	5.45 (12.0)
				1.0	215	260 (572)	3.90 (12.8)	216	5.04 (11.1)
		LF/0		1.4	188	261 (575)	4.45 (14.6)	186-208	4.86 (10.7)
				1.3	187	242 (534)	4.33 (14.2)	222	5.45 (12.0)
		0/LF		1.4	190	267 (588)	4.42 (14.5)	198	5.08 (11.2)
30/1		LF/LF		1.4	185	263 (579)	3.96 (13.0)	180-209	5.36 (11.8)
				1.3	189	272 (600)	3.90 (12.8)	188-226	5.27 (11.6)
				1.2	202	275 (606)	3.87 (12.7)	194	5.40 (11.9)
				1.0	216	233-263 (513-580)	3.96-4.64 (13.0-15.2)	209-275	5.08 (11.2)
			>0	1.0	217	257 (567)	3.96 (13.0)	232	4.90 (10.8)
			<0	1.0	217	256 (564)	3.96 (13.0)	234-264	4.86 (10.7)

TABLE 2.- AIRCRAFT CONFIGURATIONS AND FLIGHT CONDITIONS - Concluded

Wake generating aircraft, B-747								Wake probe aircraft, Learjet	
Flaps, deg	Gear	Thrust	β, deg	C_L	V, knots	W×10^{-3}, kg (lb)	h×10^{-3}, m (ft)	V, knots	W×10^{-3}, kg (lb)
30/1		LF/0	0	1.3	188	238 (525)	4.45 (14.6)	203	5.22 (11.5)
				1.2	188	236 (519)	4.42 (14.5)	178-211	5.08 (11.2)
		0/LF		1.3	188	241 (530)	4.45 (14.6)	195-236	5.36 (11.8)
				1.2	188	235 (517)	4.45 (14.6)	204	5.08 (11.2)
	Down	LF/LF		1.4	183	256 (563)	3.90 (12.8)	192-213	5.22 (11.5)
				1.3	183	253 (557)	3.90 (12.8)	190	5.13 (11.3)
				0.9	219	252 (556)	3.90 (12.8)	219	5.04 (11.1)

TABLE 3.- AIRCRAFT CHARACTERISTICS AND AERODYNAMIC COEFFICIENTS ABOUT THE BODY AXES OF THE LEARJET WITH FLAPS AT 20°

C_{ℓ_β} = -0.00180-0.000083α, 1/deg

$C_{\ell_{\delta_a}}$ = 0.00114, 1/deg

$C_{\ell_{\delta_r}}$ = 0.00041, 1/deg

C_{ℓ_p} = -0.00850, 1/deg

C_{ℓ_r} = 0.00338 + 0.000335α, 1/deg

C_{m_α} = -0.0190, 1/deg

$C_{m_{\delta_e}}$ = -0.0225, 1/deg

C_{m_q} = -0.209, 1/deg

C_{n_β} = 0.00200 - 0.000043α, 1/deg

$C_{n_{\delta_a}}$ = -0.00010, 1/deg

$C_{n_{\delta_r}}$ = -0.00130, 1/deg

C_{n_p} = -0.00064 - 0.000229α, 1/deg

C_{n_r} = -0.00480, 1/deg

C_{N_α} = 0.0909, 1/deg

C_{Y_β} = -0.0116, 1/deg

b = 10.4 m (34.1 ft)

c = 2.1 m (7.04 ft)

S = 21.6 m^2 (232 ft^2)

$\delta_{a_{max}}$ = 36.4 deg

$\delta_{e_{max}}$ = 15 deg

$\delta_{r_{max}}$ = 30 deg

Figure 1.- Boeing 747 wake generator aircraft.

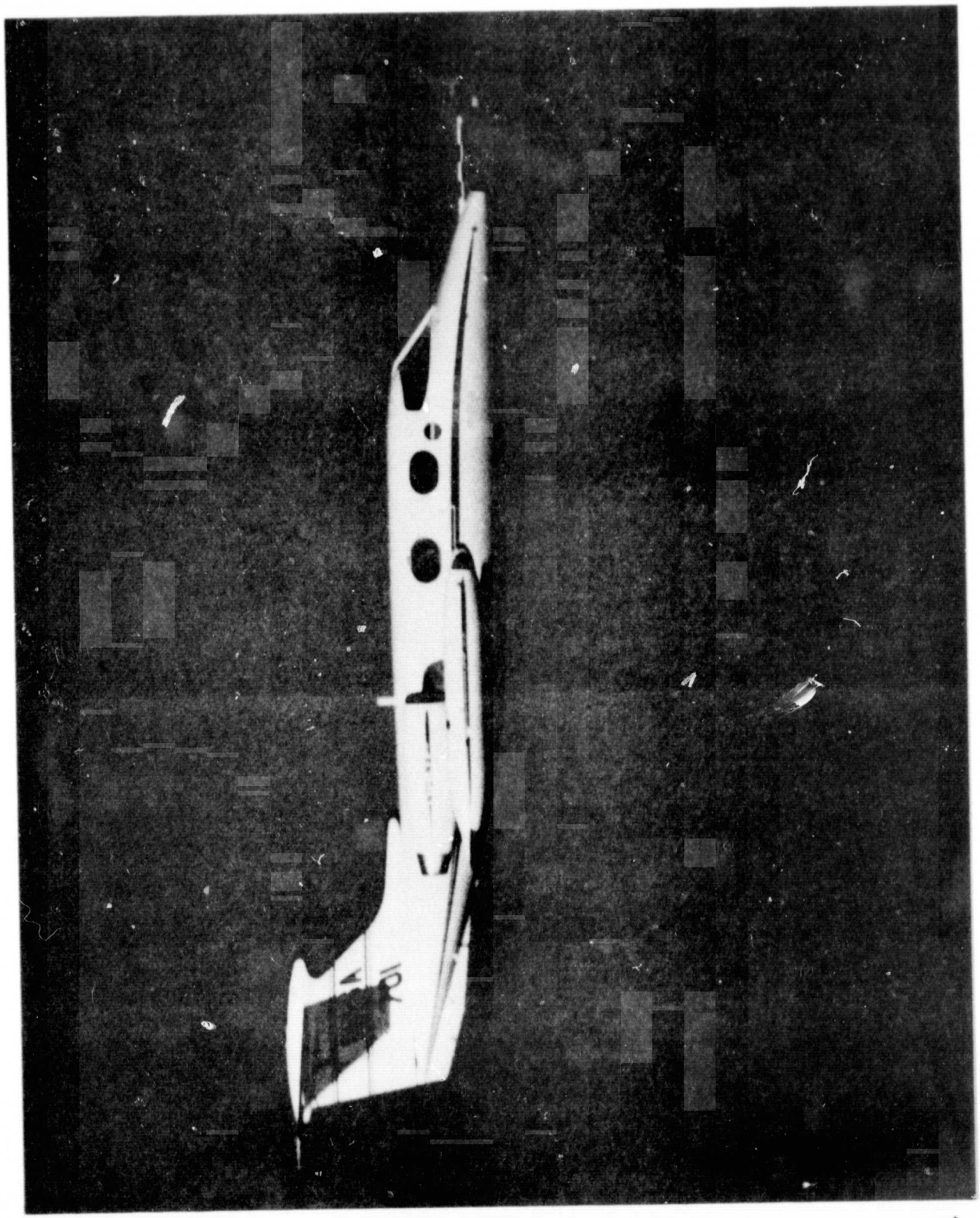

Figure 2.- Learjet probe aircraft.

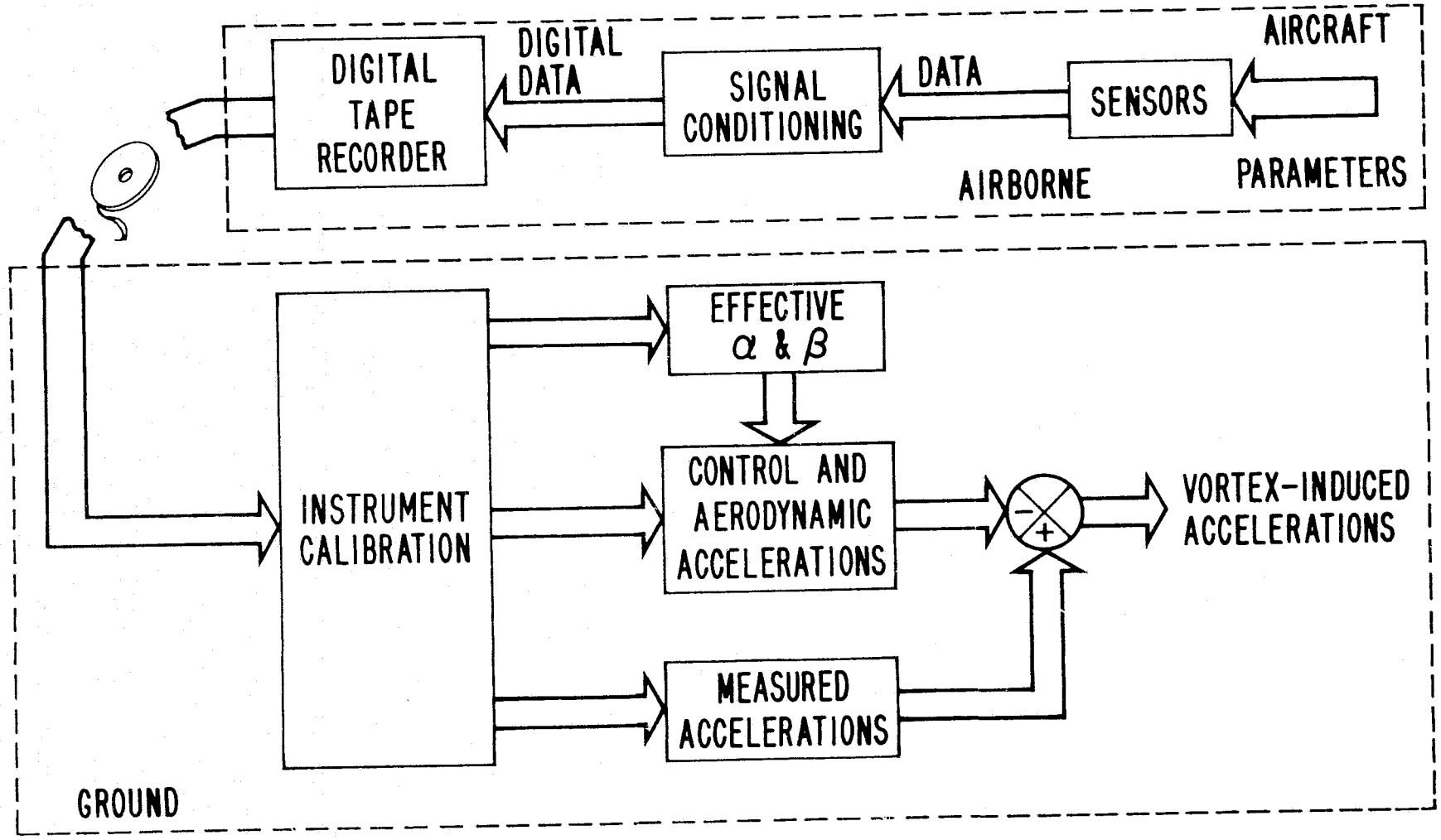

Figure 3.- Block diagram of data-reduction system used for upset measurements.

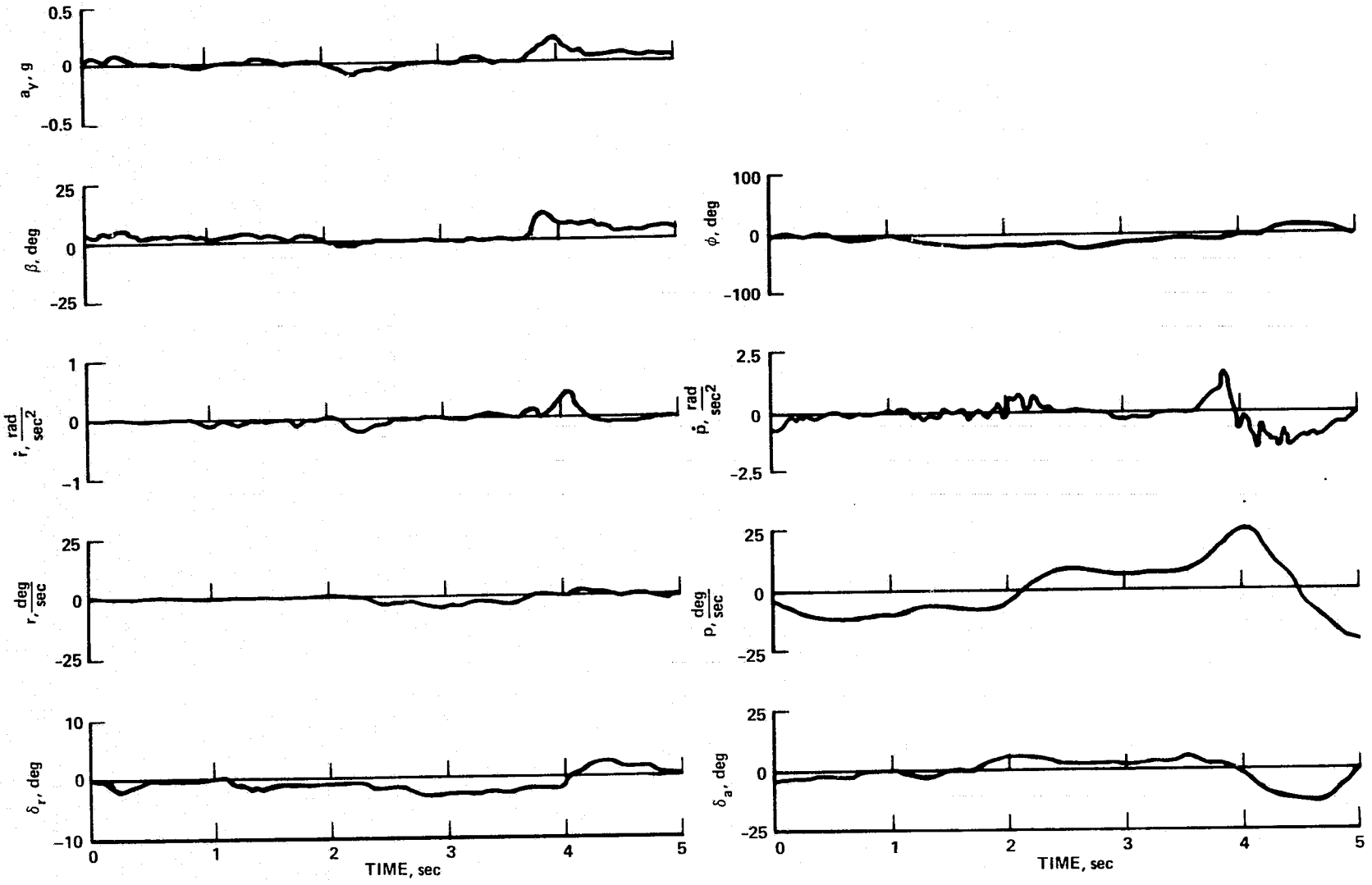

(a) Lateral-directional.

Figure 4.- Time histories of the Learjet responses to the B-747 wake vortex; separation distance - 8.7 km (4.7 n. mi.); B-747 with flaps down, gear up, thrust for level flight.

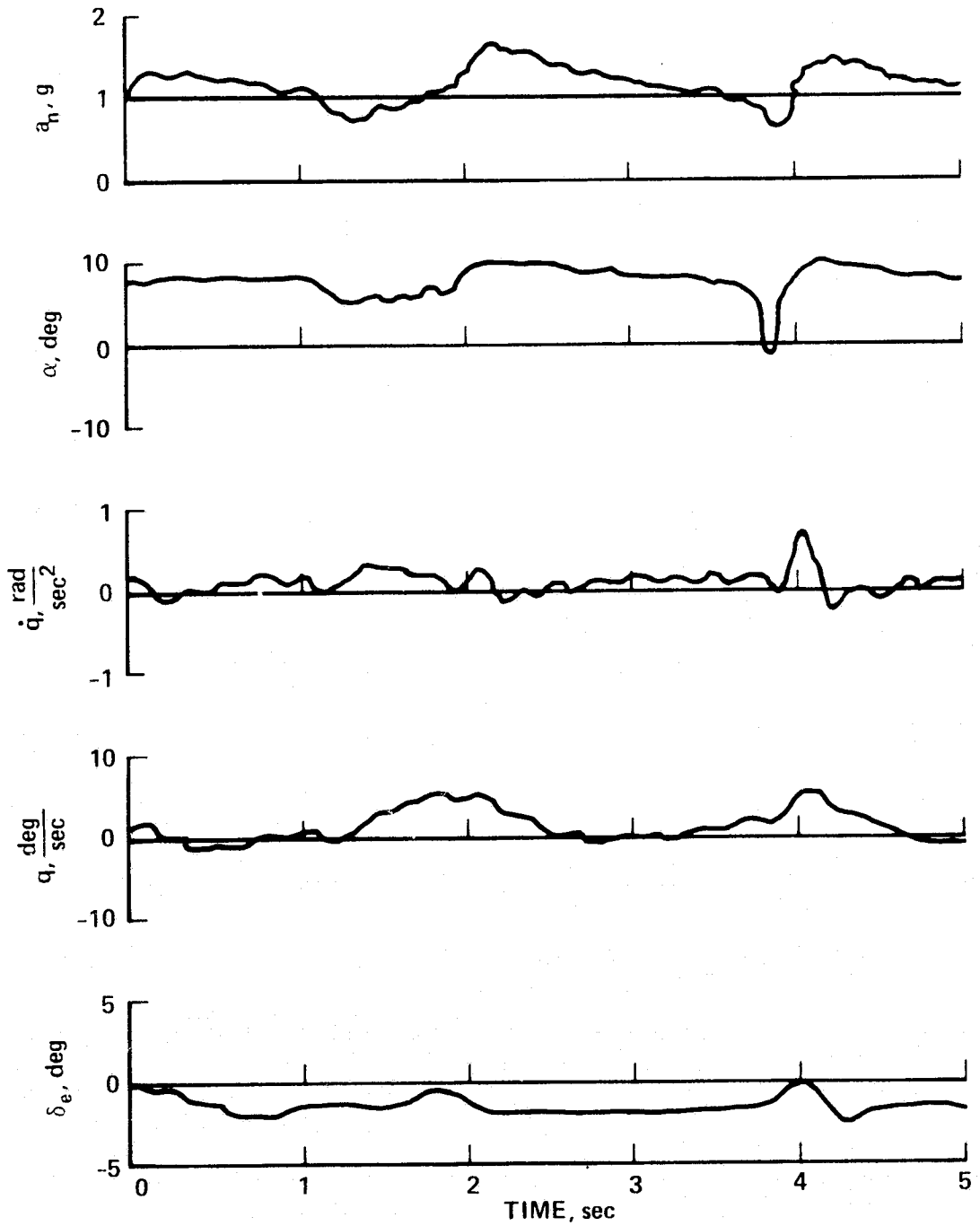

(b) Longitudinal.

Figure 4.- Concluded.

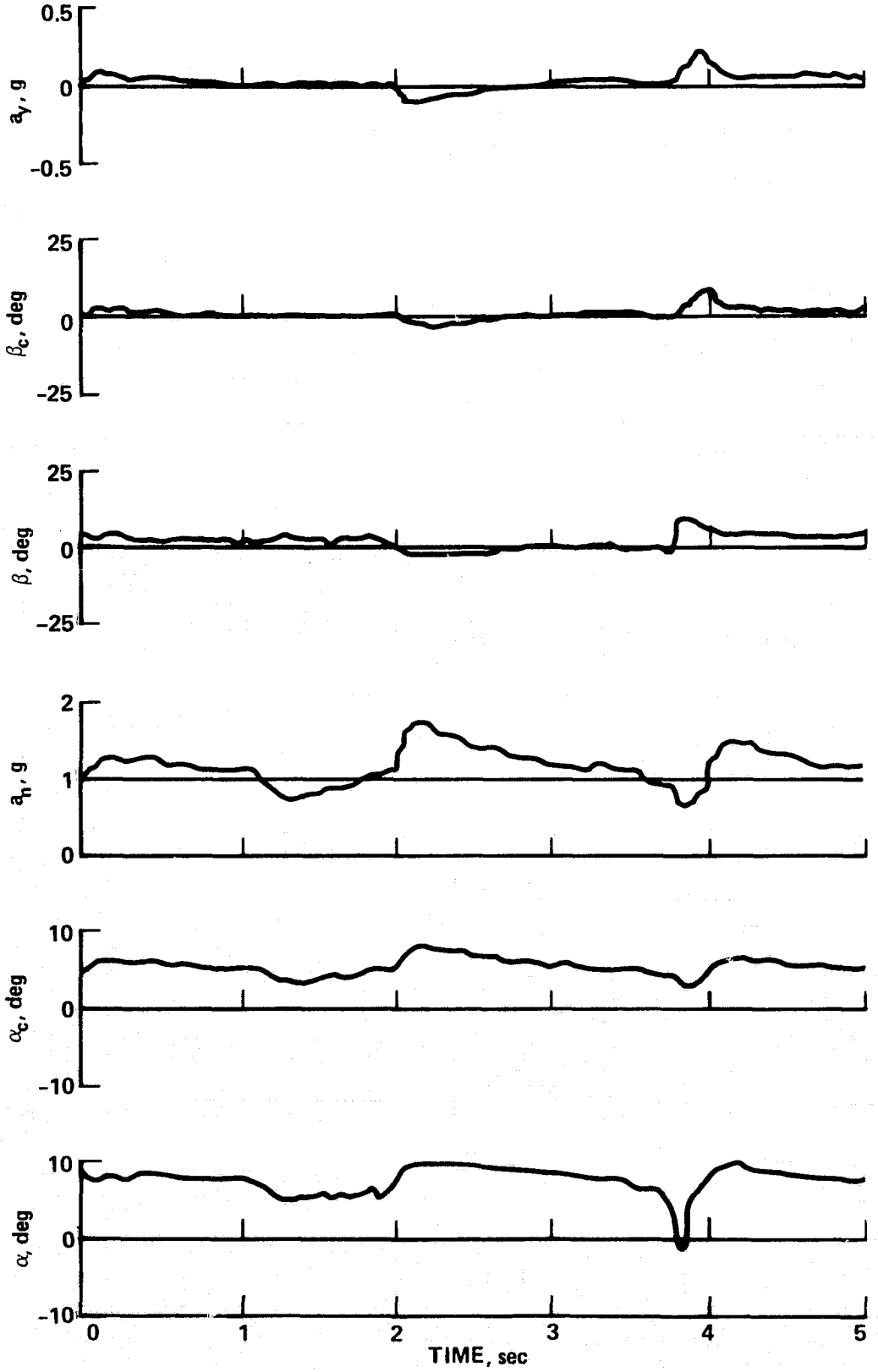

Figure 5.- Comparison of calculated values with measured values of sideslip angle and angle of attack.

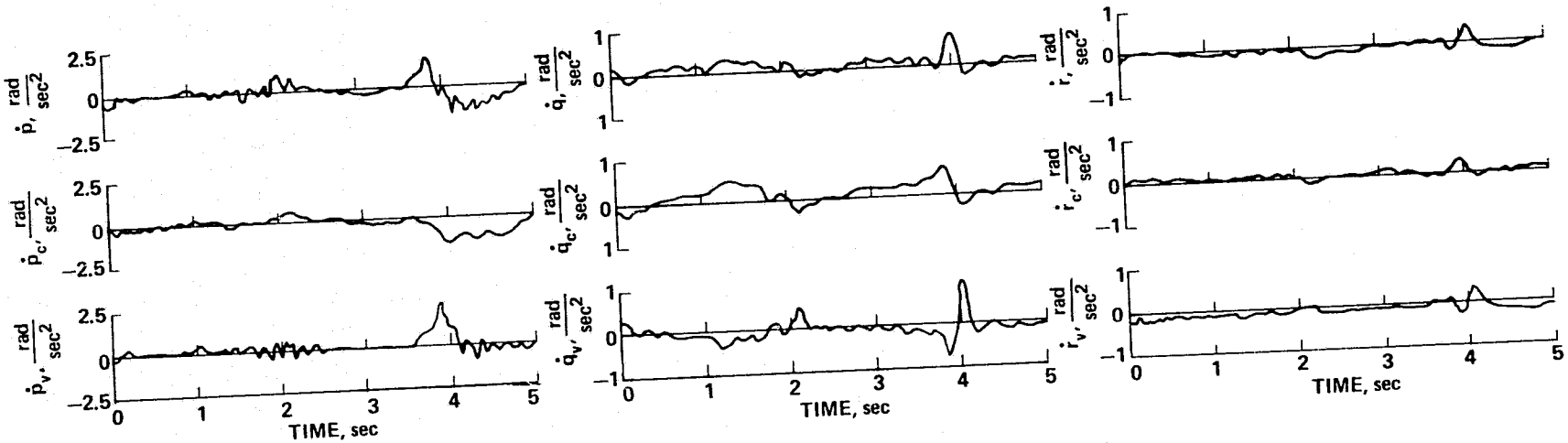

Figure 6.- Comparison of measured, calculated, and vortex-induced accelerations.

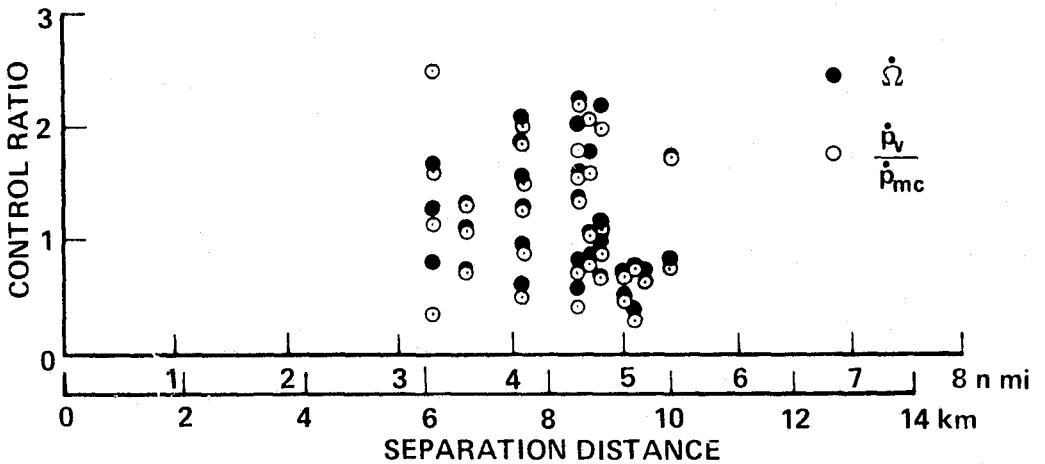

Figure 7.- Comparison of Learjet total spin control and rolling-moment control ratios; B-747 with flaps down 30/30, gear up, thrust for level flight, C_L = 1.4.

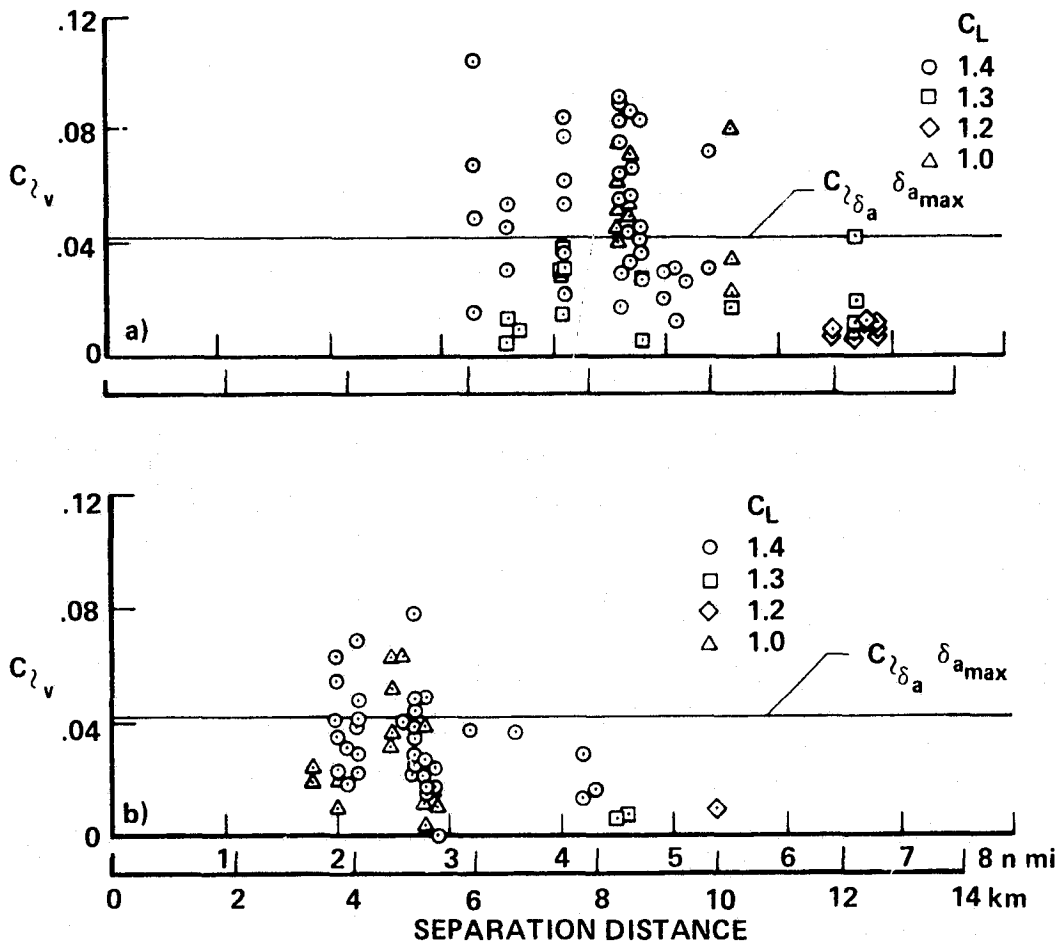

(a) Learjet rolling-moment coefficient; B-747 with flaps down 30/30, gear up, thrust for level flight.

(b) Learjet rolling-moment coefficient; B-747 with outboards flaps up 30/1, gear up, thrust for level flight.

Figure 8.- Effect of B-747 lift coefficient.

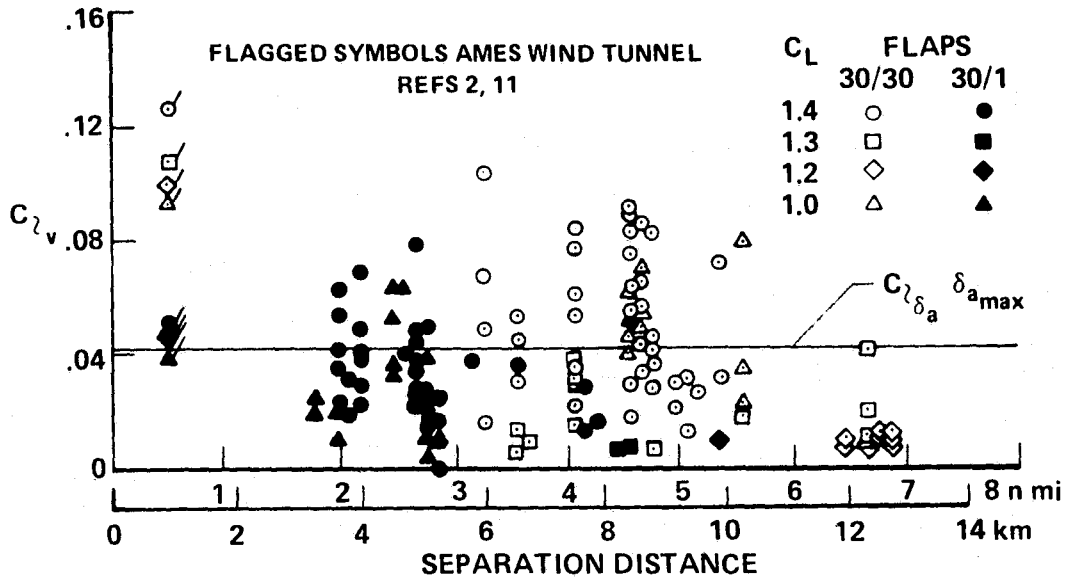

Figure 9.- Effect of B-747 flap configuration; B-747 with gear up, thrust for level flight.

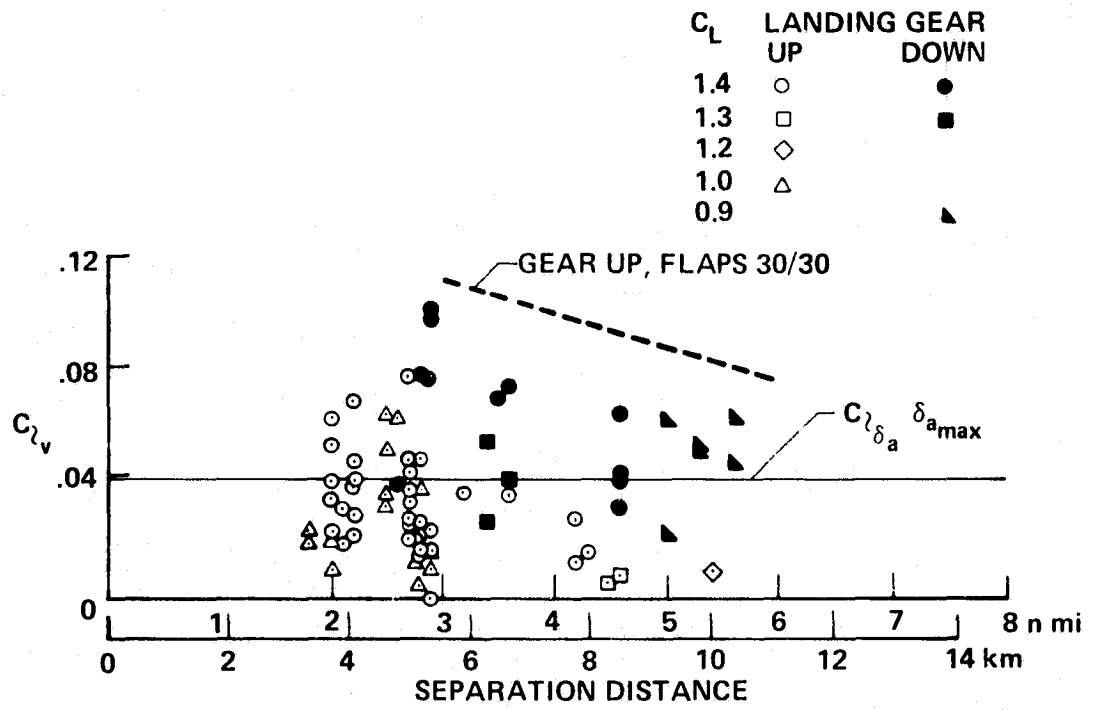

Figure 10.- Effect of B-747 landing gear; B-747 with outboard flaps up 30/1, thrust for level flight.

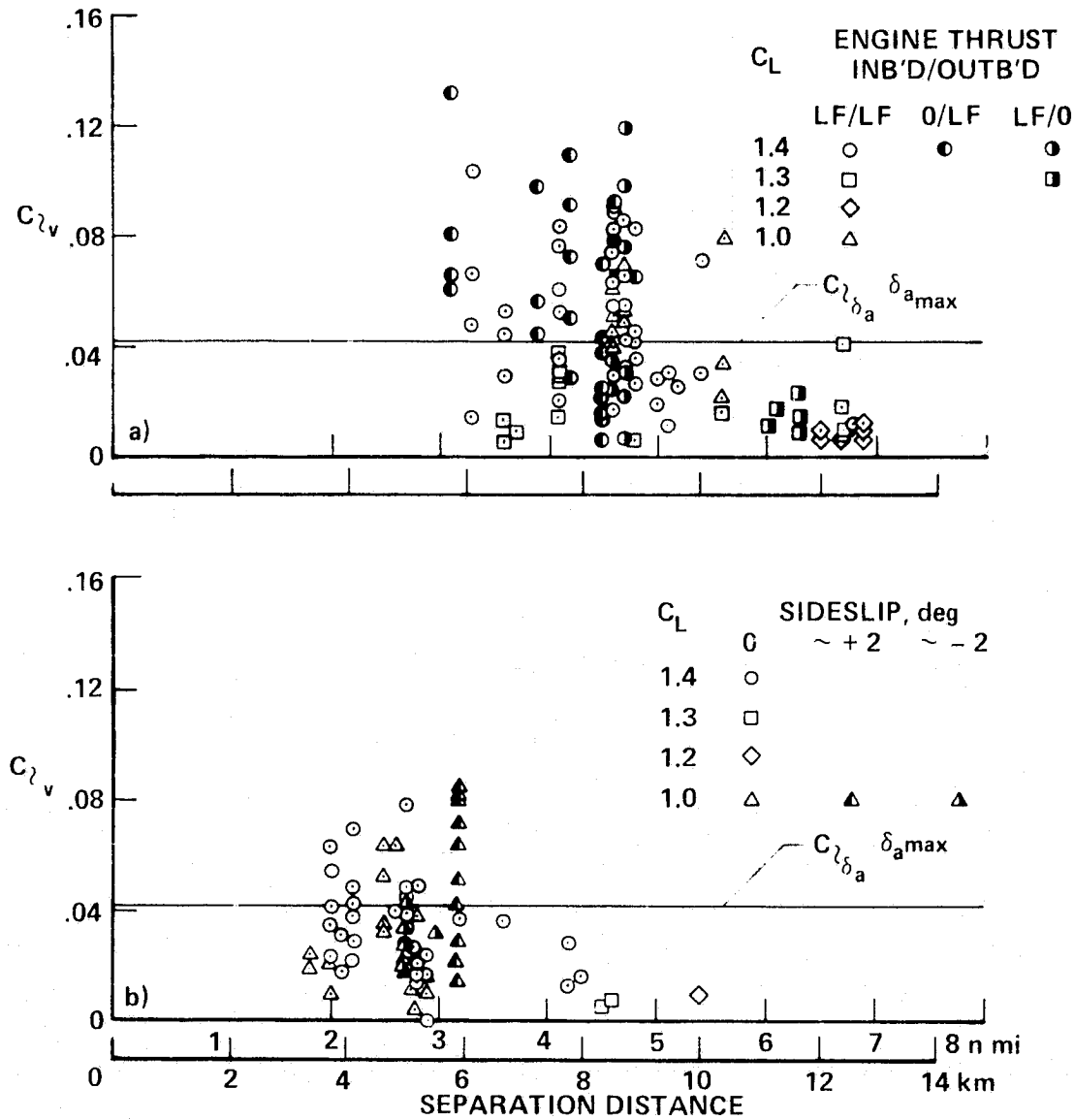

(a) B-747 with flaps down 30/30, gear up.
(b) B-747 with outboard flaps up 30/1, gear up.

Figure 11.- Effect of B-747 engine thrust.

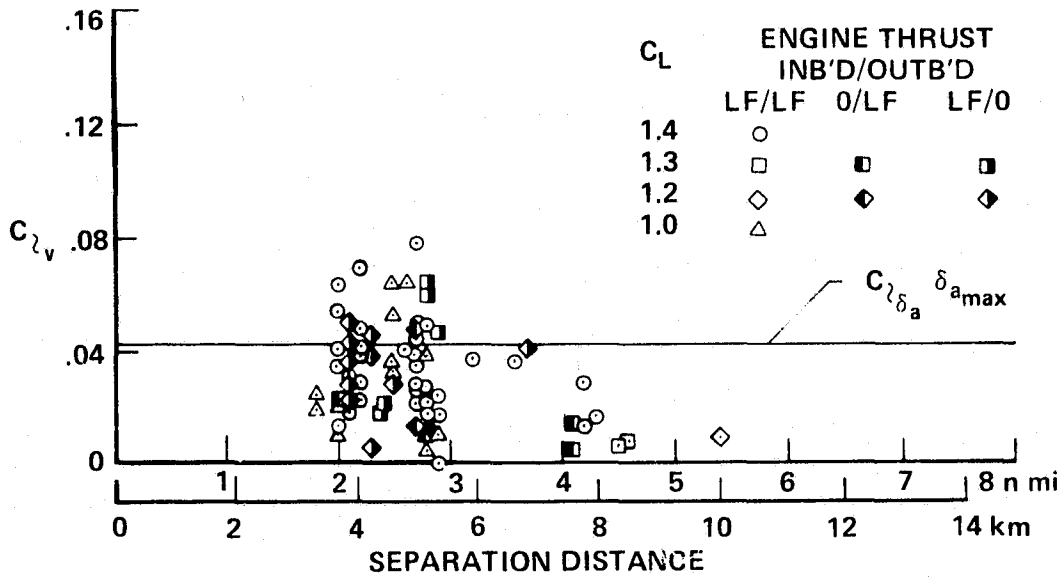

Figure 12.- Effect of B-747 sideslip; B-747 with outboard flaps up 30/1, gear up, thrust for level flight.

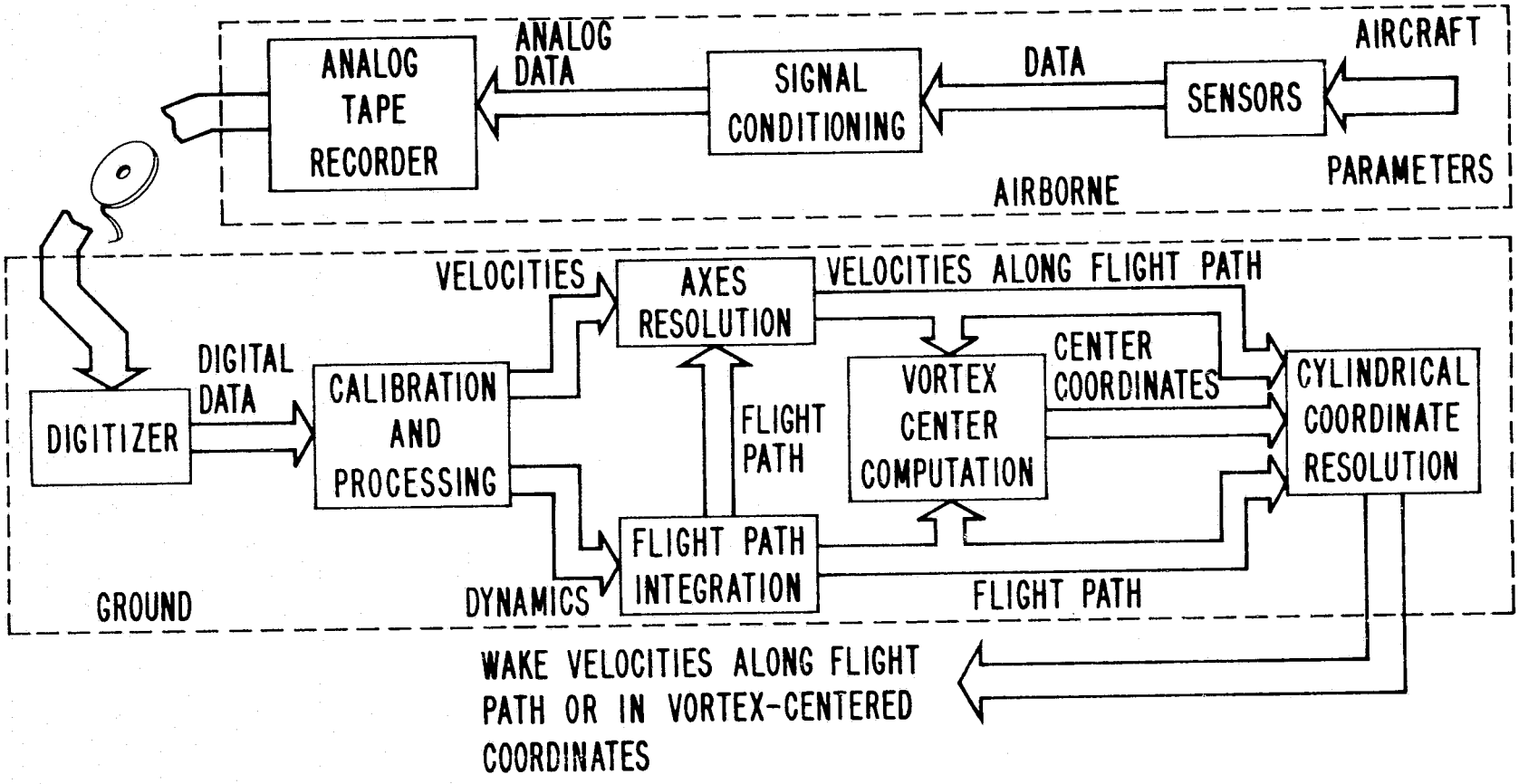

Figure 13.- Block diagram of data-reduction system used for velocity profile measurements.

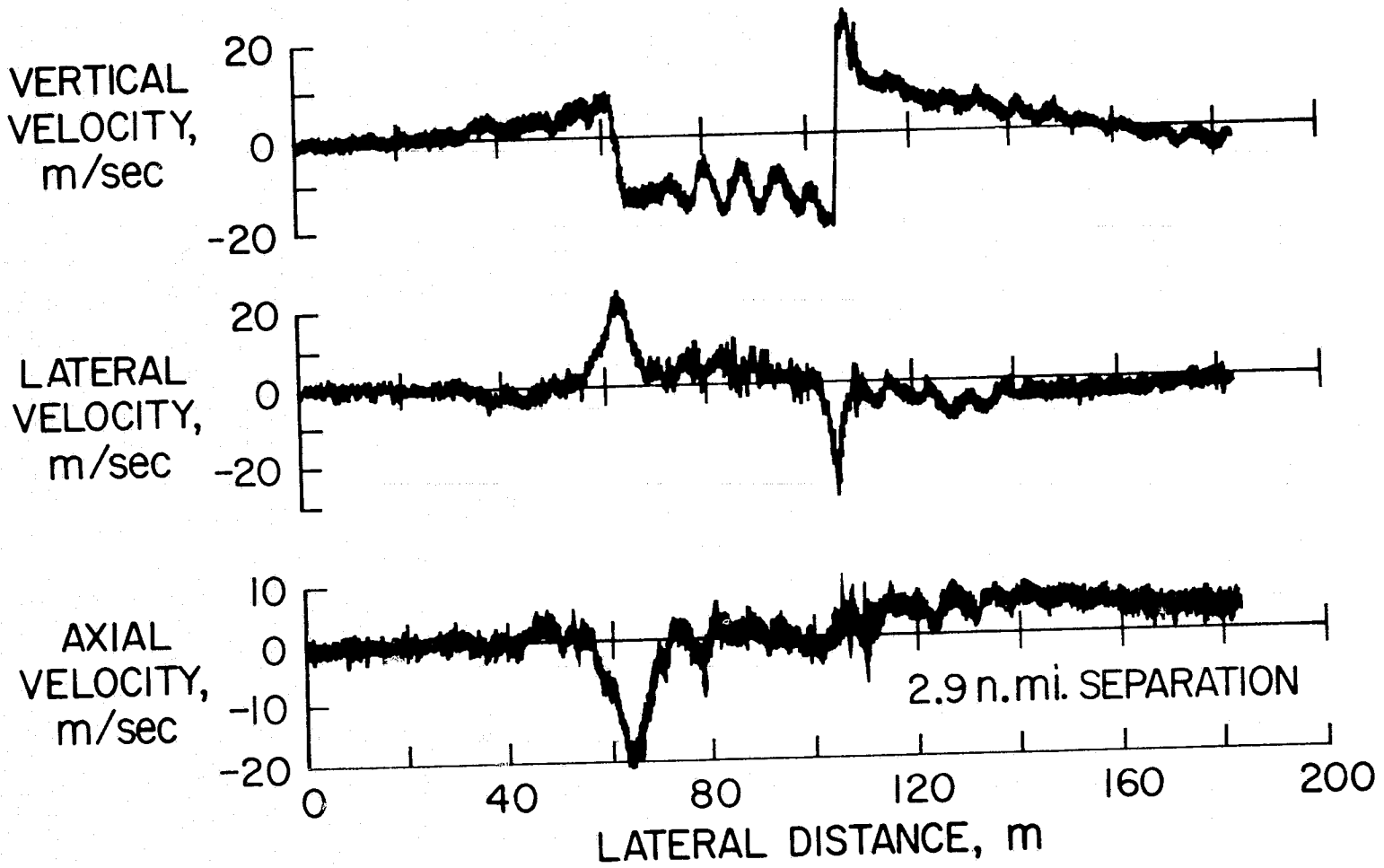

Figure 14.- Vertical, lateral, and axial velocity components in the wake of a B-747 in normal landing configuration.

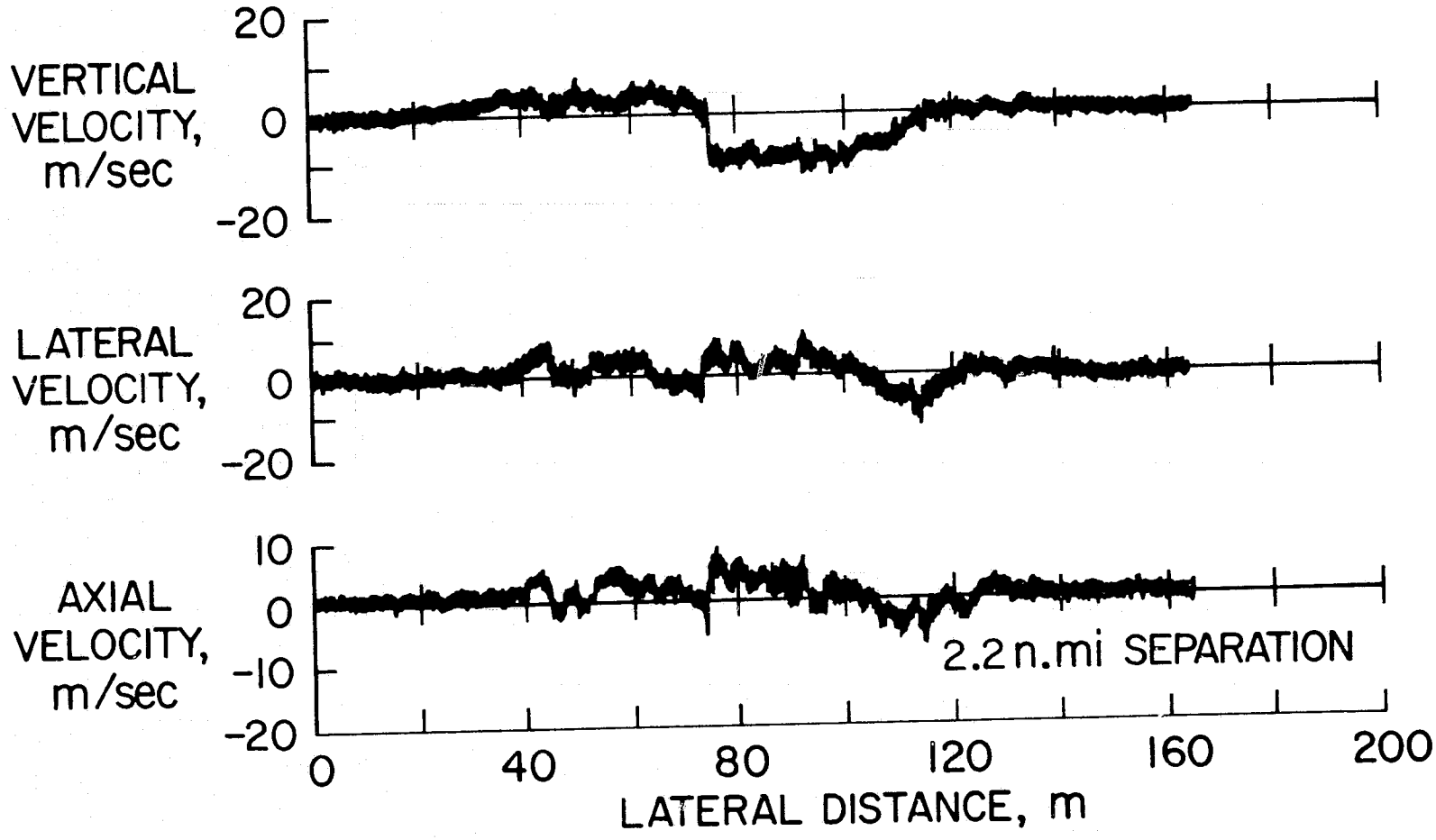

Figure 15.- Vertical, lateral, and axial velocity components in the wake of a B-747 with outboard flap retracted.

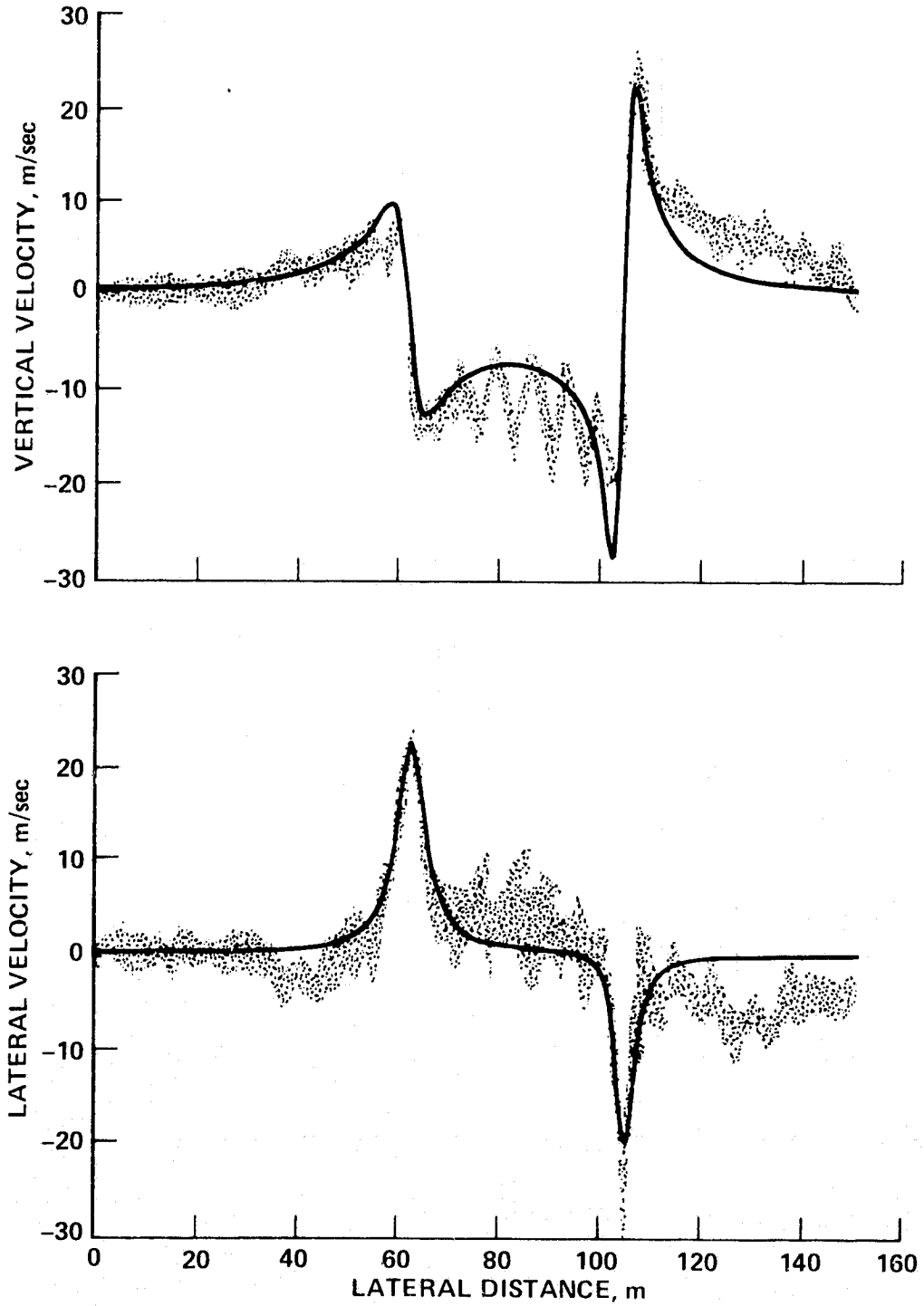

Figure 16.- Velocity components resulting from a mathematical model of a Lamb vortex pair matched to the data of figure 14.

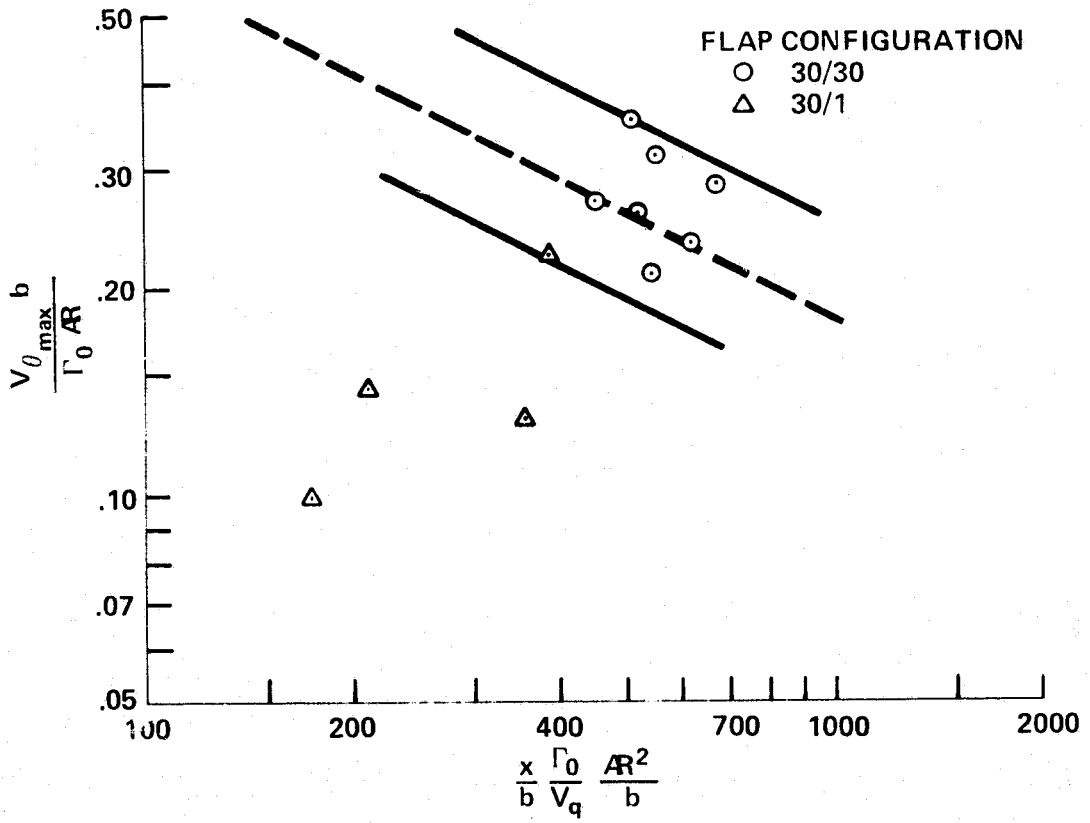

Figure 17.- Peak tangential velocity as a function of downstream distance.

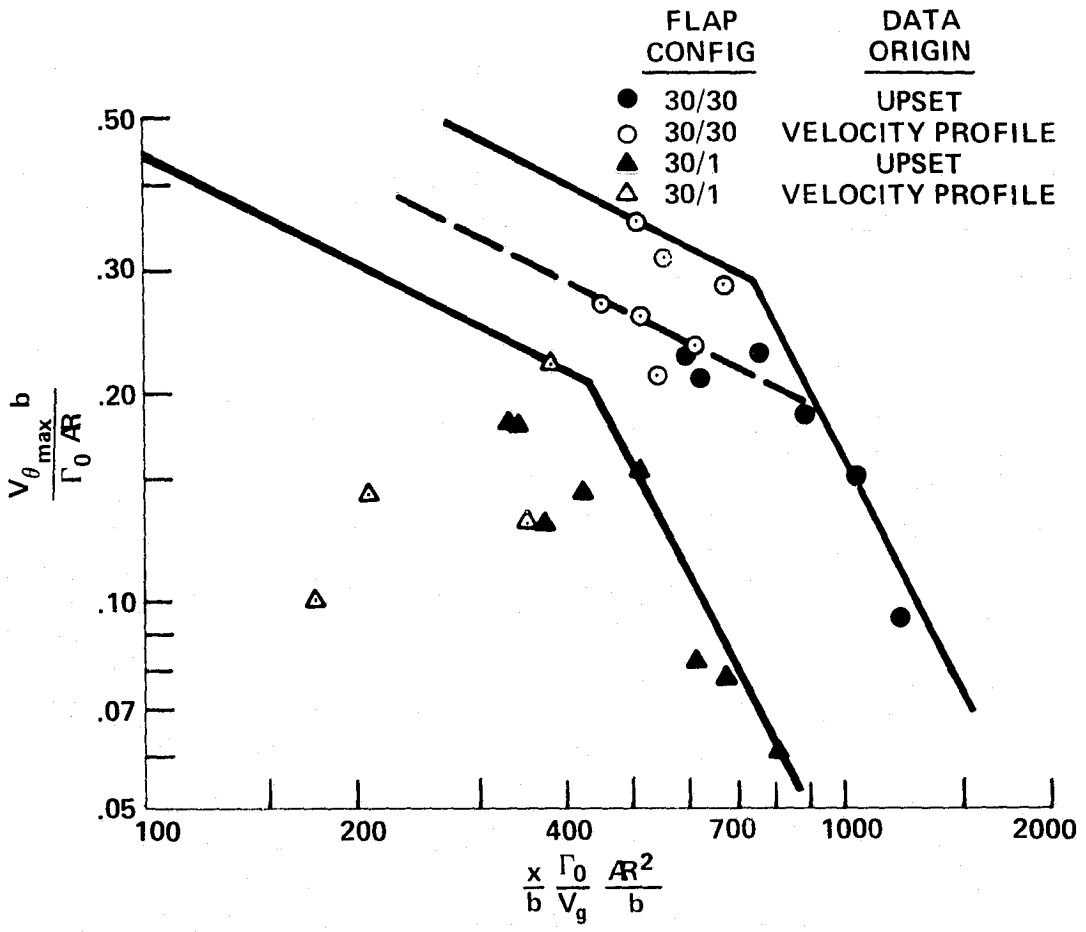

Figure 18.- Comparison of peak tangential velocities derived from upset measurements with those from velocity profile measurements.

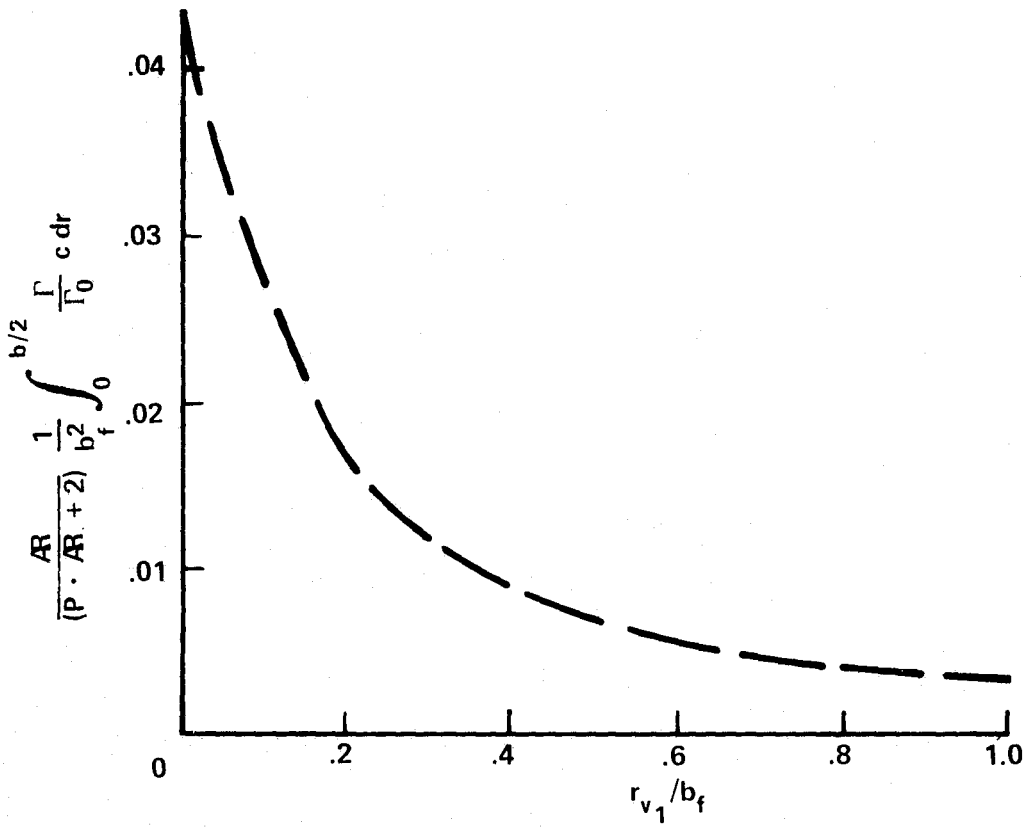

Figure 19.- Evaluation of parameter used in relating rolling moments to maximum vortex induced velocity. Curve for Learjet wing planform.

1. Report No.	2. Government Accession No.	3. Recipient's Catalog No.
NASA TM-73,263		

4. Title and Subtitle	5. Report Date
A FLIGHT INVESTIGATION OF THE WAKE TURBULENCE ALLEVIATION RESULTING FROM A FLAP CONFIGURATION CHANGE ON A B-747 AIRCRAFT	6. Performing Organization Code
7. Author(s) Robert A. Jacobsen and Barbara J. Short	8. Performing Organization Report No. A-7116
9. Performing Organization Name and Address Ames Research Center Moffett Field, California 94035	10. Work Unit No. 505-08-22 11. Contract or Grant No.
12. Sponsoring Agency Name and Address National Aeronautics and Space Administration Washington, D. C. 20546	13. Type of Report and Period Covered Technical Memorandum 14. Sponsoring Agency Code

15. Supplementary Notes

16. Abstract

A flight test investigation has been conducted to evaluate the effects of a flap configuration change on the vortex wake characteristics of a Bocing 747 (B-747) aircraft as measured by differences in upset response resulting from deliberate vortex encounters by a following Learjet aircraft and by direct measurement of the velocities in the wake. The flaps of the B-747 have a predominant effect on the wake. The normal landing flap configuration produces a strong vortex that is attenuated when the outboard flap segments are raised; however, extension of the landing gear at that point increases the vortex-induced upsets. These effects are in general agreement with existing wind tunnel and flight data for the modified flap configuration; however, the previously measured adverse effects of increased lift coefficient and idle thrust are not readily evident.

17. Key Words (Suggested by Author(s))	18. Distribution Statement
Wake vortex Vortex hazard Trailing vortices	Unlimited STAR Category - 03

19. Security Classif. (of this report)	20. Security Classif. (of this page)	21. No. of Pages	22. Price*
Unclassified	Unclassified	44	$4.00

*For sale by the National Technical Information Service, Springfield, Virginia 22161